LETTER

doi:10.1038/nature12583

The maize Gα gene *COMPACT PLANT2* functions in CLAVATA signalling to control shoot meristem size

Peter Bommert[1], Byoung Il Je[1], Alexander Goldshmidt[1]† & David Jackson[1]

Shoot growth depends on meristems, pools of stem cells that are maintained by a negative feedback loop between the *CLAVATA* pathway and the *WUSCHEL* homeobox gene[1]. CLAVATA signalling involves a secreted peptide, CLAVATA3 (CLV3)[2], and its perception by cell surface leucine-rich repeat (LRR) receptors, including the CLV1 receptor kinase[3] and a LRR receptor-like protein, CLV2 (ref. 4). However, the signalling mechanisms downstream of these receptors are poorly understood, especially for LRR receptor-like proteins, which lack a signalling domain[5]. Here we show that maize *COMPACT PLANT2* (*CT2*) encodes the predicted α-subunit (Gα) of a heterotrimeric GTP binding protein. Maize *ct2* phenotypes resemble *Arabidopsis thaliana clavata* mutants, and genetic, biochemical and functional assays indicate that CT2/Gα transmits a stem-cell-restrictive signal from a CLAVATA LRR receptor, suggesting a new function for Gα signalling in plants. Heterotrimeric GTP-binding proteins are membrane-associated molecular switches that are commonly activated by ligand binding to an associated seven-pass transmembrane (7TM) G-protein-coupled receptor (GPCR)[6]. Recent studies have questioned the idea that plant heterotrimeric G proteins interact with canonical GPCRs[7], and our findings suggest that single pass transmembrane receptors act as GPCRs in plants, challenging the dogma that GPCRs are exclusively 7TM proteins.

The *ct2* reference allele *(ct2-Ref)* was obtained from the Maize Genetics Stock Center and introgressed into various inbred lines. It showed strong expressivity in B73, which we used for phenotypic characterization. *ct2* mutants displayed a range of phenotypes, including a shorter stature (Fig. 1a and Extended Data Fig. 1a, b), and shorter and wider leaves (Extended Data Table 1). *ct2* shoot apical meristems (SAMs) were also wider, with an average diameter of 134 μm (± 6.8) compared to 109 μm (± 5.8, $n = 15$; P value = 0.001; Student's t test) for normal siblings (Extended Data Fig. 1c, d). Despite the larger SAM, its identity and organization appeared normal in *ct2*, as shown by *in situ* hybridization with *KNOTTED1* (Extended Data Fig. 1e–h)[8].

ct2 mutants also had striking inflorescence defects, including strongly fasciated ears (Fig. 1b, c) and thicker tassel branches (Fig. 1g, h), with a higher density of flower bearing structures known as spikelets (Extended Data Fig. 1k, l), resembling maize *CLAVATA* receptor mutants[9,10]. To analyse inflorescence development, we used scanning electron microscopy (SEM). In wild type, the inflorescence meristem initiates spikelet pair meristems (SPMs) in a regular phyllotaxy, and SPMs branch to generate a pair of spikelet meristems in adjacent vertical rows, corresponding to rows of seeds in the cob (Fig. 1d and Extended Data Fig. 1i). When *ct2* ears were approximately 2 mm in length, the inflorescence meristem was enlarged (Fig. 1e and Extended Data Fig. 1j), leading to extra rows of SPMs, and meristem enlargement became more severe during development (Fig. 1f). *ct2* tassel meristems were also abnormally enlarged (Fig. 1i, j).

ct2 mapped to the short arm of Chromosome 1 (http://www.maizegdb.org), and using ~1,000 *ct2-Ref* F_2 mutants, we fine mapped it to a 1.2 megabase pair (Mbp) region containing approximately 30 genes. Among these was one encoding the α-subunit of a heterotrimeric GTP protein (Fig. 2a). Based on similar dwarf phenotypes in rice Gα mutants[11], we sequenced the locus from *ct2-Ref*, and found a 126 bp insertion within exon 14 (Fig. 2b). Three additional *ct2* alleles were isolated using a targeted ethylmethane sulphonate (EMS) screen, and each contained transition mutations in conserved splice sites, causing aberrant splicing

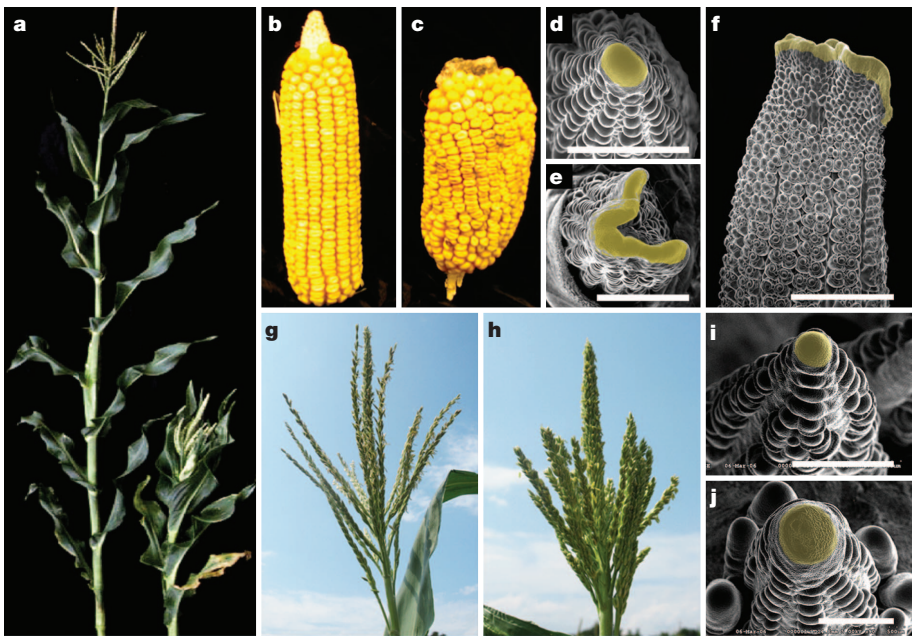

Figure 1 | *ct2* mutant phenotypes. **a,** *ct2* mutants (right) are semi-dwarfed, compared to wild-type sib. **b, c,** Wild-type (**b**) and *ct2* (**c**) ear showing fasciation. **d,** Top-down view of a wild-type ear primordium, the inflorescence meristem is shaded in yellow. **e,** *ct2* ear primordium showing enlargement and fasciation. **f**, Older *ct2* ear is more fasciated. **g,** Wild-type tassel. **h**, *ct2* tassel has as a thicker appearance due to increased spikelet density. **i**, Top-down view of a wild-type tassel inflorescence meristem (shaded). **j,** *ct2* tassel shows enlarged inflorescence meristem (shaded). Scale bars represent 1 mm (**d**, **e**), 2 mm (**f**) and 500 μm (**i**, **j**).

[1]Cold Spring Harbor Laboratory, Cold Spring Harbor, New York 11724, USA. †Present address: Monsanto Company, 700 Chesterfield Parkway, Chesterfield, Missouri 63017, USA.

(Fig. 2b and Extended Data Fig. 2a). Each mutation was predicted to introduce premature stop codons, suggesting they are null alleles. Our characterization of four independent alleles indicates that *ct2* encodes the Gα subunit of a predicted heterotrimeric G protein.

We next expressed a CT2 fusion with yellow fluorescent protein (YFP) driven by the *CT2* endogenous promoter. This fusion complemented *ct2* mutants (Extended Data Fig. 2b–f), and CT2–YFP was observed in a thin line at the cell periphery that co-localized with an FM4-64 plasma membrane counterstain after plasmolysis (Fig. 2c, d). CT2–YFP also showed co-localization with FM4-64 in the SAM (Fig. 2e), and was expressed throughout the SAM and developing leaf primordia (Fig. 2f, g), and in the inflorescence meristem, where it was enriched in the outer layers (Fig. 2h and Extended Data Fig. 3a). Expression persisted throughout spikelet and floral development (Extended Data Fig. 3b–e). We also detected CT2–YFP expression in roots, again along the cell periphery, consistent with its predicted plasma membrane localization (Extended Data Fig. 3f). In summary, CT2–YFP appeared to localize to plasma membranes in meristems and in developing organs.

As the *ct2* inflorescence phenotypes were reminiscent of other maize fasciated ear mutants[9,10], we analysed genetic interactions between *ct2* and *thick tassel dwarf1* (*td1*) or *fasciated ear2* (*fea2*), which encode maize orthologues of *CLV1* and *CLV2*, respectively. To obtain a quantitative measure of phenotypic strength, we counted spikelet density in double mutant segregating families, as in other studies[9,10]. Spikelet density of *ct2-Ref; td1-Ref* double mutants was significantly higher than either single mutant (P value = 0.0001; Student's t test), indicating an additive genetic effect and suggesting *ct2* and *td1* act in different pathways. In contrast, spikelet density in *ct2-Ref; fea2-0* double mutants was not significantly different from that of the *ct2* single mutants (P value = 0.42; Student's t test), even though each single mutant was significantly higher than normal (P value = 0.001; Student's t test) (Extended Data Fig. 4). This genetic interaction suggests they act in a common pathway. To substantiate these findings, we measured SAM diameter in *ct2-Ref; fea2-0* double mutant segregating families. In the double mutants, SAM diameter was not significantly different from that of *fea2-0* single mutants (P value = 0.41; Student's t test), even though each single mutant was significantly higher than normal (P value = 0.001; Student's t test) (Fig. 3a). This genetic interaction indicates that *fea2* is epistatic to *ct2* with respect to SAM diameter, and suggests they act in a common pathway. However, *ct2* mutant meristems were significantly smaller than the double mutants (Fig. 3a), suggesting that FEA2 signals through other pathways in addition to CT2/Gα to control SAM size.

To investigate the molecular basis for the epistatic interaction, we made a peptide antiserum against FEA2, and used a GFP antiserum to detect CT2–YFP. The anti-FEA2 antiserum detected a protein with an apparent weight of ~75 kDa, slightly increased compared to its predicted 61 kDa, in extracts from wild type (B73) but not *fea2* mutant ears, indicating that it was specific (Fig. 3b). Treatment with PNGaseF showed that FEA2, like many other LRR receptors, is glycosylated[12], and aqueous two-phase partitioning showed that it is predominantly present in the plasma membrane (Extended Data Fig. 5b, c). We also detected a band of the predicted size in total, soluble and membrane enriched extracts from CT2–YFP plants, but not from non-transgenic (B73) plants, and CT2–YFP was enriched in membrane fractions (Fig. 3c and Extended Data Fig. 5d). FEA2 and CT2 were found in overlapping higher molecular weight native complexes (Extended Data Fig. 6), and we used extracts from the CT2–YFP maize lines for immunoprecipitation experiments. Membrane-enriched extracts were immunoprecipitated using anti-GFP antiserum and following stringent washing the immunoprecipitate was probed by western blotting. We detected FEA2 in the input, and also in the immunoprecipitated fraction, suggesting that FEA2 interacts with CT2 (Fig. 3d and Extended Data Fig. 5e). We used a different membrane-localized fusion protein, PIN1–YFP[13], as a control, and FEA2 was not detected in the immunoprecipitated fraction, nor was it detected in controls using wild type B73 extracts

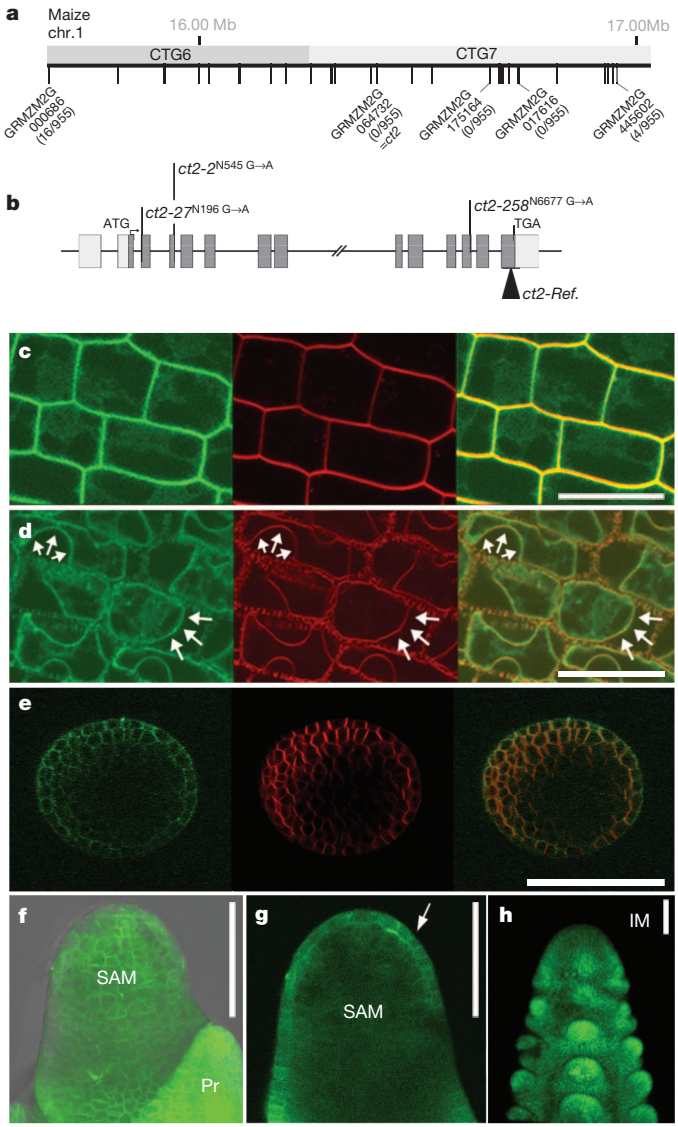

Figure 2 | Cloning and expression of *CT2*. **a**, Positional cloning of *ct2*. Numbers of recombinants/F_2 individuals indicated. Vertical lines represent gene models. **b**, *ct2* gene, exons shown as grey boxes and different alleles are marked. **c**, Leaf cells expressing CT2–YFP (green), counterstained with FM4-64 (red), visible as a thin line around the cell. Overlay (right). **d**, Following plasmolysis, CT2–YFP (arrows) remains co-localized with FM4-64. **e**, Two-photon images of SAM expressing CT2–YFP, counterstained with FM4-64. **f**, CT2-YFP expression throughout the SAM and leaf primordium (Pr). **g**, Confocal section shows L1 layer enrichment. **h**, CT2–YFP in immature ears. Three-dimensional reconstructions are shown in **f** and **h**. Scale bars, 100 μm.

(Fig. 3d and Extended Data Fig. 5e). These data indicate that CT2 interacts specifically with FEA2 *in vivo*, and together with their epistatic genetic interaction supports the hypothesis that CT2 signals in a FEA2 receptor pathway.

Our data suggest that CT2/Gα functions in a CLAVATA signalling pathway. To further test this hypothesis, we asked if *ct2* mutants show altered sensitivity to the CLV3 ligand. CLV3 function can be assessed by adding exogenous peptide, which inhibits meristem growth[14]. Maize seedling shoot meristems are covered by leaf primordia, so we used embryos, where the SAM is exposed. Wild-type embryos grew normally in culture in the presence of a control, scrambled CLV3 peptide (sCLV3), but SAM growth was strongly inhibited in the presence of CLV3 (Fig. 3e). *ct2* mutant embryos also grew normally in the presence of sCLV3, but showed a significantly reduced sensitivity to CLV3 (Fig. 3e), supporting the idea that CT2 is involved in transmitting a

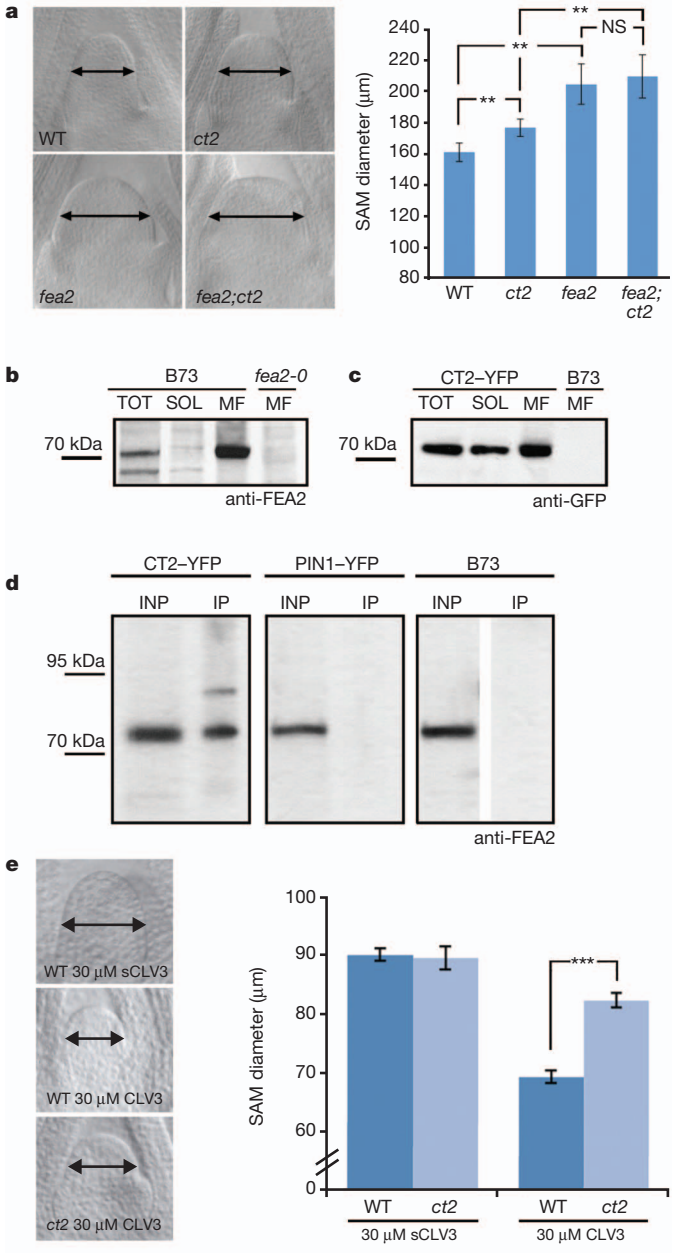

Figure 3 | Interactions between CT2 and CLAVATA signalling. **a**, Cleared SAMs; SAM diameter in double mutants was not significantly different from *fea2-0* (P value = 0.41; Student's t test; $n = 10$). Error bars represent s.d. NS, not significant; WT, wild type. $^{**}P = 0.001$. **b**, Western blot showing anti-FEA2 specificity; a band is seen in wild-type (B73) total extracts (TOT) and membrane fractions (MF), but not in soluble (SOL), or *fea2-0*. **c**, CT2–YFP detection using anti-GFP. **d**, CT2 and FEA2 co-immunoprecipitate; a band is detected in co-immunoprecipitates using CT2–YFP, but not in PIN1–YFP or B73 controls. Experiments were conducted with 3 biological replicates. INP, total input. **e**, Embryos cultured with CLV3 or scrambled peptide (sCLV3). Wild-type SAM growth is strongly inhibited by CLV3, but *ct2* is significantly less inhibited ($^{***}P$ value = 0.0001; Student's t test; $n = 10$ for each genotype). Error bars represent s.e., experiments were conducted with 3 biological replicates.

CLV3-derived signal. Together with our findings that maize *ct2* mutants are strongly fasciated, similar to *CLV* mutants, *ct2* and *fea2* act in a common genetic pathway, and CT2 and FEA2 proteins interact *in vivo*, we suggest that CT2/Gα acts to transmit CLAVATA-dependent signals to control shoot stem cell proliferation. This finding helps explain the conundrum that FEA2, like CLV2 and other receptor-like proteins are receptors without a signalling domain. Although it was proposed that *CORYNE* (*CRN*) might signal downstream of CLV2 (ref. 15), this idea has been questioned by the finding that CRN lacks kinase activity[5].

No obvious meristem size phenotype has been described for Gα mutants in other plants, although inducible expression of *Arabidopsis* Gα led to production of ectopic shoot meristems[16]. A possible explanation for the stronger meristem phenotype in maize is that the ear has undergone recent intense selection for increased size and kernel row number[17,18] and may be more sensitive to genetic perturbation. Alternatively, the relative importance of Gα signalling, or the contribution of parallel pathways with overlapping function(s), may vary between species.

The idea that Gα interacts with the single pass transmembrane receptor FEA2 is at odds with the dogma from yeast and mammalian systems that it interacts with G-protein-coupled receptors, which are seven pass transmembrane proteins[19]. To ask if this change might be a general phenomenon in plants, we performed mass spectroscopic analysis of proteins immunoprecipitated using CT2–YFP, and found additional predicted LRR receptor proteins as candidate CT2–YFP interactors, and we did not detect any 7TM proteins (Extended Data Table 1). However, based solely on proteomic data it is difficult to rule out the possibility that a 7TM protein acts as an intermediate between FEA2 and CT2. Indeed, plants contain 7TM receptors[20], and it is possible that such a protein is in a FEA2–CT2 complex, although their role as GPCRs has been questioned[7]. For example, biochemical and structural data suggests that plant Gα proteins are self-activating, supporting the idea that they do not interact with canonical 7TM receptors[7]. In some instances, plant Gα proteins are regulated by 7TM regulator of G protein signalling (RGS) proteins. However, such proteins appear to be missing from the grasses, suggesting that Gα regulatory mechanisms differ even within the plant kingdom[7].

Plant Gα genes control a wide array of phenotypes, including responses to hormones, drought, pathogens, vegetative growth, flower and panicle development[21]. *Arabidopsis* heterotrimeric G proteins have overlapping functions with the LRR receptor-like kinase *ERECTA* (*ER*), including flower and leaf development and cell division[22,23]. Double mutant analysis of *er* and *agb1*, which encodes the β-subunit of the heterotrimeric G protein, revealed that *ERECTA* and *AGB1* likely function in the same pathway in regulating fruit shape[22]. Therefore, as supported by our proteomic data, heterotrimeric G proteins might be involved in signalling downstream of other LRR receptors, which are extremely abundant in plants[24].

METHODS SUMMARY

Plant growth and map based cloning. Maize plants were grown in the field or in the greenhouse. Phenotyping used the *ct2-Ref* allele introgressed 5 times into the B73 inbred line. Then 1,000 mutants from a segregating F_2 population were used for map-based cloning, and additional alleles were identified using targeted EMS mutagenesis (Extended Data Fig. 2a). Scanning electron microscopy was performed on fresh tissue using a Hitachi S-3500N SEM, as described[10].

Double mutants were constructed and analysed after genotyping and meristem sizes were measured using cleared tissues.

Transgenic lines and analysis. The CT2–YFP transgene was constructed by amplification of genomic fragments and fusing the YFP gene in-frame at an internal position, and transformed into maize (for primer sequences see Methods). For confocal microscopy, tissues were dissected and counterstained with 1 mg ml^{-1} FM4-64 solution (Molecular Probes) in water for 1 min then washed with water and imaged within 5 min. For plasmolysis, leaf epidermal tissues were peeled, placed in FM4-64 solution, washed with water twice, and imaged. Subsequently, the tissues were incubated for 5–10 min with 30% glycerol and imaged again. Two-photon images were taken with a custom-made two-photon microscope.

Protein detection and co-immunoprecipitation assays were performed using standard techniques (see Methods).

CLV3 peptide assays. Maize embryos segregating for the *ct2* mutation were dissected at ~10 days after pollination, when the SAM was exposed, and cultured on gel media[25] containing CLV3 peptide (RTVPSGPDPLHH; 30 µg ml^{-1}; Genscript) or scrambled peptide (PPTRGLSHHPVD; 30 µg ml^{-1}). After 10 days, embryos were harvested for genotyping, and fixed in FAA (formalin, 45%, acetic acid, 10%, ethanol, 45%) and cleared in methyl salicylate, and meristems measured by

microscopy. Experiments used at least 10 embryos per genotype, and were replicated in triplicate.

Online Content Any additional Methods, Extended Data display items and Source Data are available in the online version of the paper; references unique to these sections appear only in the online paper.

Received 17 January; accepted 20 August 2013.
Published online 11 September 2013.

1. Stahl, Y. & Simon, R. Plant primary meristems: shared functions and regulatory mechanisms. *Curr. Opin. Plant Biol.* **13,** 53–58 (2010).
2. Fletcher, J. C., Brand, U., Running, M. P., Simon, R. & Meyerowitz, E. M. Signaling of cell fate decisions by *CLAVATA3* in *Arabidopsis* shoot meristems. *Science* **283,** 1911–1914 (1999).
3. Clark, S. E., Williams, R. W. & Meyerowitz, E. M. The *CLAVATA1* gene encodes a putative receptor kinase that controls shoot and floral meristem size in *Arabidopsis. Cell* **89,** 575–585 (1997).
4. Jeong, S., Trotochaud, A. E. & Clark, S. E. The *Arabidopsis CLAVATA2* gene encodes a receptor-like protein required for the stability of the CLAVATA1 receptor-like kinase. *Plant Cell* **11,** 1925–1934 (1999).
5. Nimchuk, Z. L., Tarr, P. T. & Meyerowitz, E. M. An evolutionarily conserved pseudokinase mediates stem cell production in plants. *Plant Cell* **23,** 851–854 (2011).
6. Assmann, S. M. G proteins Go green: a plant G protein signaling FAQ sheet. *Science* **310,** 71–73 (2005).
7. Urano, D. *et al.* G protein activation without a GEF in the plant kingdom. *PLoS Genet.* **8,** e1002756 (2012).
8. Jackson, D., Veit, B. & Hake, S. Expression of maize *KNOTTED1* related homeobox genes in the shoot apical meristem predicts patterns of morphogenesis in the vegetative shoot. *Development* **120,** 405–413 (1994).
9. Bommert, P. *et al. thick tassel dwarf1* encodes a putative maize ortholog of the *Arabidopsis CLAVATA1* leucine-rich repeat receptor-like kinase. *Development* **132,** 1235–1245 (2005).
10. Taguchi-Shiobara, F., Yuan, Z., Hake, S. & Jackson, D. The *fasciated ear2* gene encodes a leucine-rich repeat receptor-like protein that regulates shoot meristem proliferation in maize. *Genes Dev.* **15,** 2755–2766 (2001).
11. Ashikari, M., Wu, J., Yano, M., Sasaki, T. & Yoshimura, A. Rice gibberellin-insensitive dwarf mutant gene *Dwarf 1* encodes the α-subunit of GTP-binding protein. *Proc. Natl Acad. Sci. USA* **96,** 10284–10289 (1999).
12. van der Hoorn, R. A. *et al.* Structure-function analysis of Cf-9, a receptor-like protein with extracytoplasmic leucine-rich repeats. *Plant Cell* **17,** 1000–1015 (2005).
13. Gallavotti, A., Yang, Y., Schmidt, R. J. & Jackson, D. The relationship between auxin transport and maize branching. *Plant Physiol.* **147,** 1913–1923 (2008).
14. Fiers, M. *et al.* The 14-amino acid CLV3, CLE19, and CLE40 peptides trigger consumption of the root meristem in *Arabidopsis* through a *CLAVATA2*-dependent pathway. *Plant Cell* **17,** 2542–2553 (2005).
15. Müller, R., Bleckmann, A. & Simon, R. The receptor kinase CORYNE of *Arabidopsis* transmits the stem cell-limiting signal CLAVATA3 independently of CLAVATA1. *Plant Cell* **20,** 934–946 (2008).
16. Ullah, H. *et al.* Modulation of cell proliferation by heterotrimeric G protein in *Arabidopsis. Science* **292,** 2066–2069 (2001).
17. Bommert, P., Nagasawa, N. S. & Jackson, D. Quantitative variation in maize kernel row number is controlled by the *FASCIATED EAR2* locus. *Nature Genet.* **45,** 334–337 (2013).
18. Brown, P. J. *et al.* Distinct genetic architectures for male and female inflorescence traits of maize. *PLoS Genet.* **7,** e1002383 (2011).
19. Katritch, V., Cherezov, V. & Stevens, R. C. Structure-function of the G protein-coupled receptor superfamily. *Annu. Rev. Pharmacol. Toxicol.* **53,** 531–556 (2013).
20. Pandey, S., Nelson, D. C. & Assmann, S. M. Two novel GPCR-type G proteins are abscisic acid receptors in *Arabidopsis. Cell* **136,** 136–148 (2009).
21. Perfus-Barbeoch, L., Jones, A. M. & Assmann, S. M. Plant heterotrimeric G protein function: insights from *Arabidopsis* and rice mutants. *Curr. Opin. Plant Biol.* **7,** 719–731 (2004).
22. Lease, K. A. *et al.* A mutant *Arabidopsis* heterotrimeric G-protein β subunit affects leaf, flower, and fruit development. *Plant Cell* **13,** 2631–2641 (2001).
23. Shpak, E. D., Berthiaume, C. T., Hill, E. J. & Torii, K. U. Synergistic interaction of three ERECTA-family receptor-like kinases controls *Arabidopsis* organ growth and flower development by promoting cell proliferation. *Development* **131,** 1491–1501 (2004).
24. Shiu, S. H. & Bleecker, A. B. Plant receptor-like kinase gene family: diversity, function, and signaling. *Sci. STKE* **2001,** re22 (2001).
25. Iyer-Pascuzzi, A. S. *et al.* Imaging and analysis platform for automatic phenotyping and trait ranking of plant root systems. *Plant Physiol.* **152,** 1148–1157 (2010).

Supplementary Information is available in the online version of the paper.

Acknowledgements The authors thank T. Mulligan for plant care; T. Rocheford for growing the *ct2* targeted EMS screens; F. Albeanu for help with two-photon microscopy; P. Yin for assistance with genotyping; K. Rivera and D. Pappin for performing proteomic experiments; and T. Zadrozny, Q. Wu and W. Boss for assistance and advice with two-phase partitioning. P.B. was supported by DFG grant Bo 3012/1-1, A.G. was supported by the BARD Postdoctoral award no FI-431-2008, B.I.J was supported by Dupont-Pioneer (CSHL-Collaborative agreement), P.B. and D.J. were supported by the National Science Foundation Plant Genome Program, DBI-0604923.

Author Contributions P.B., B.I.J., A.G. and D.J. designed experiments and analysed data; P.B. performed all experiments, except peptide assays and contributions to imaging, phenotyping and biochemical assays (B.I.J.) and fluorescence imaging (A.G.); and P.B. and D.J. wrote the paper.

Author Information Reprints and permissions information is available at www.nature.com/reprints. The authors declare no competing financial interests. Readers are welcome to comment on the online version of the paper. Correspondence and requests for materials should be addressed to D.J. (jacksond@cshl.edu).

METHODS

Plant growth, map based cloning and Isolation of additional alleles. Maize plants were grown in the field or in the greenhouse. Phenotyping used the *ct2-Ref* allele introgressed 5 times into the B73 inbred line. 1,000 mutants from a segregating F_2 population were used for map-based cloning. To isolate additional *ct2* alleles, *ct2* heterozygous plants were crossed using EMS treated wild-type pollen, and a total of 33,000 M1 plants were screened for *ct2* phenotypes (Extended Data Fig. 2a)[26].

Meristem imaging and *in situ* hybridization. Scanning electron microscopy was performed on fresh tissue using a Hitachi S-3500N SEM, as described[10]. *In situ* hybridization experiments were performed as described[8].

CT2–YFP transgene construction and imaging. The CT2–YFP transgene was constructed by amplification of genomic fragments and fusing the YFP gene in-frame at an internal position, and transformed into maize. We used the MultiSite Gateway System (Invitrogen) as described[27]. All fragments were amplified using Phusion *Taq* polymerase (Finnzymes) and transferred to the pTF101 Gateway compatible maize transformation vector by the multisite LR recombination reaction (Invitrogen). The coding region of YFP was inserted between the two amino-terminal α helices, αA and αB, of CT2, because insertion of GFP at the same position in GPA1 produces a functional fusion that rescues the *gpa1* mutation[28]. Confirmed clones were transferred to *Agrobacterium* and transformed into maize, as described[27]. Primers are listed in the Methods. To determine whether the CT2–YFP construct could complement the *ct2-Ref* allele, primary CT2–YFP transformants were crossed as males to heterozygous *ct2-Ref* mutant females. F_1 plants that contained the CT2–YFP transgene were backcrossed by homozygous *ct2-Ref* mutants. Transgenic plants of these families were randomly sib-crossed and resulting families subsequently analysed for complementation. For genotyping, a 5′ 1.9 kb fragment of the *ct2*-gene was amplified and digested with AccI, as a single nucleotide polymorphism causes a loss of the 5′ AccI site in the *ct2-Ref* allele. DNA from B73 and A188 inbred lines were also used as control templates, because A188 × B73 hybrid stocks were used for transformation. The 1.9 kb PCR fragment also contains the site of the YFP insertion, which allows for parallel PCR detection of the transgene. The presence of the transgene locus was additionally monitored by Basta-treatment of leaf tips[29].

For confocal microscopy, tissues were dissected and counterstained with 1 mg ml^{-1} FM4-64 solution (Molecular Probes) in water for 1 min then washed with water and imaged within 5 minutes. Images were taken with a Zeiss LSM 710 microscope, using 514 nm laser excitation and 520–560 nm emission for detection of the YFP and 585–750 nm emission for detection of FM4-64. *Z*-stack images were reconstructed using Bitplane Imaris 7 software. For plasmolysis, leaf epidermal tissues were peeled, placed in FM4-64 solution, washed with water twice and imaged. Subsequently, the tissues were incubated for 5–10 min with 30% glycerol and imaged again. Two-photon images were taken with a custom made two-photon microscope using a Chameleon Ultra II femtosecond pulsed laser tuned at 930 nm. A 505–550 bandpass filter was used for detection of the YFP fluorescence emission and a 575–635 bandpass filter for FM4-64 fluorescence emission.

Double mutant analysis. Double mutants were constructed and analysed after genotyping. Double mutant segregating families were scored for spikelet density by counting the number of spikelets in a 5 cm region of the tassel central spike, after 2 cm had been removed from the tip. To measure meristem size at the time of the inflorescence transition, shoot apical meristems of ~28-day-old plants were dissected, cleared and measured as described previously[10].

Protein extraction, PNGaseF assay, detection and co-immunoprecipitation assays. Total protein was extracted by grinding developing maize ears (~1–2 cm) in liquid nitrogen. The powder was resuspended in twice the volume of extraction buffer (50 mM Tris, pH 7.5, 150 mM NaCl, 10% glycerol, protease inhibitor mix (Roche), according to the manufacturer's instructions), filtered through four layers of Miracloth, and centrifuged at 4,000*g* for 10 min at 4 °C. To separate the microsomal (membrane) fraction the extract was centrifuged at 100,000*g* for 1 h at 4 °C, and the supernatant fluid was kept as the soluble fraction. The microsomal pellet was resuspended for 30 min on ice in extraction buffer supplemented with 1% Triton X-100. Lysates were cleared by centrifugation at 4,000*g* at 4 °C for 10 min to remove non-solubilized material. An FEA2 peptide antiserum was prepared in rabbits by injection of a peptide directed against the 15 amino acids at the carboxy terminus of FEA2 (SNARNFVFRPVRVEY) and purified using peptide affinity chromatography[30]. To determine the FEA2 complex size, gel filtration was performed using a fast protein liquid chromatography system (Akta, GE) with a High Prep 16/60 Sephacryl S-300 HR column (GE). Fractions were collected every 2 ml, precipitated using trichloroacetic acid and subjected to SDS–PAGE and western blotting. Blots were probed with the anti-FEA2 peptide antibody and detected using chemiluminescence with a secondary HRP coupled antibody (GE). For CT2–YFP complex size determination, an online ultraviolet-detection HPLC system (Shimadzu LabSolutions) and a Superdex200 10/300 GL column (GE) was used. Solubilized membrane fractions were prepared as previously described, and columns were run using lysis buffer containing 150 mM NaCl, 50 mM Tris pH 7.5 and 0.1% Triton X-100. Columns were calibrated using HMW and LMW protein marker kits (GE). For the PNGaseF assay, solubilized microsomal fractions were prepared as described earlier, denatured for 10 min at 100 °C in denaturing buffer and incubated with PNGaseF (NEB) according to the manufacturer's protocol at 37 °C for 1 h. For co-immunoprecipitation experiments, solubilized microsomal fractions were incubated with 50 µl magnetic beads coupled to monoclonal mouse anti-GFP antibody (µMACs; Milteny Biotec) for 45 min at 4 °C. Flow-through columns were equilibrated using 250 µl lysis buffer before lysates were added. The MicroBead-bound target protein was magnetically separated, and washed two times with 250 µl ice-cold lysis buffer and three times with 250 µl wash buffer 1 containing 150 mM NaCl, 50 mM Tris, pH 7.5, 0.1% SDS and 0.05% IGEPAL-CA-630 (Sigma). Bound target proteins were eluted with 50 µl 1×SDS loading buffer at 95 °C. Following standard SDS–PAGE electrophoresis and western blotting, co-immunoprecipitated FEA2 protein was detected using chemiluminescence with anti-FEA2 peptide antibody and a secondary HRP-coupled antibody (GE). Co-immunoprecipitation experiments were performed three times with independent biological replicates. Aqueous two-phase partitioning was performed as described[31], using extracts from 1–4-cm maize ear primordia. Samples from the upper and lower phases, enriched for plasma membrane and endoplasmic reticulum, respectively, were probed with antisera for BiP lumenal binding protein (Agrisera AS09-481), or plasma membrane H^+ ATPase (Agrisera AS07-260), or FEA2, and detected using a secondary HRP coupled antibody (GE), according to the manufacturer's instructions.

Proteomic analysis. CT2–YFP immunoprecipitated proteins were digested by adding 25 µl of digestion buffer (2 M urea; 50 mM Tris, pH 7.5; 5 mM DTT; 2 µg trypsin). After in-column digestion for 30 min at room temperature, proteins were eluted by twice adding 50 µl of elution buffer (2 M urea; 50 mM Tris, pH 7.5; 10 mM methyl methanethiosulphonate). Digestion continued overnight at room temperature. The digestion was stopped by adding 5 µl of formic acid. One-quarter of the total volume of sample was bomb-loaded onto a C18 column and subjected to 2D MudPIT chromatography followed by mass spectrometry[32–34]. Buffers were as follows: buffer A (95% H_20, 5% ACN, 0.1% FA), buffer B (10% H_20, 90% ACN, 0.1% FA), buffer C (500 mM ammonium acetate, 5% ACN, 0.1% FA). The sample was separated online into 5 fractions, (load, 20% C, 40% C, 100% C and 90% B: 10% C) and each fraction was run over a 70 min gradient in which buffer B increased from 8% to 35%. A vented column setup with a Proxeon nano-flow HPLC pump was used to separate peptides. Peptides were then electrosprayed into an Orbitrap XL mass spectrometer using collision-induced dissociation (CID) to fragment the top 6 ions from each full mass spectrometry scan. Peaklist files were generated by Mascot Distiller (Matrix Science) and protein identification was carried out using Mascot version 2.3.

CLV3 peptide assays. Maize embryos segregating for the *ct2* mutation were dissected at ~10 days after pollination, when the SAM was exposed, and cultured on gel media[25] containing CLV3 peptide (RTVPSGPDPLHH; 30 µg ml^{-1}; Genscript) or scrambled peptide (PPTRGLSHHPVD; 30 µg ml^{-1}). After 10 days; embryos were harvested for genotyping, and fixed in FAA (formalin, 45%, acetic acid, 10%, ethanol, 45%) and cleared in methyl salicylate, and meristems measured by microscopy. Experiments used at least 10 embryos per genotype, and were replicated in triplicate.

Primer sequences. *attb4-ct2-Fo*: 5′-GGGGACAACTTTGTATAGAAAAGTTGCCTACCAGGGCAGGCTTTAT-3′; *attb1-ct2-Re*: 5′-GGGGACTGCTTTTTTGTACAAACTTGCGGCTAACTCTTTAGCTCCCTCAT-3′; *attb2-ct2-Fo*: 5′-GGGGACAGCTTTCTTGTACAAAGTGGGACAAGTGGAACCAGATTCTTCAA-3′; *attb3-ct2-Re*: 5′-GGGGACAACTTTGTATAATAAAGTTGAGGACTGCTGCTTCATCCAG-3′; *ct2-Ref-Fo*: 5′-TGAGGAGCTCTACTTCCAAAGC-3′; *ct2-Ref-Re*: 5′-TGGCTTATAACACCACATCCTC-3′; *ct2-258-Fo*: 5′-CGGACAAATGGTGTGGTAGA-3′; *ct2-258-Re*: 5′-CTCGTCGATCAGCTTGAATG-3′; *ct2-Acc-Fo*: 5′-ACCCGAACCCTAACCTAAGC-3′; *ct2-Acc-Re*: 5′-GAGGATAATTGTGTACCTTTGTCG-3′.

26. Freeling, M. & Walbot, V. *The Maize Handbook*. (Springer-Verlag, 1994).
27. Mohanty, A. *et al.* Advancing cell biology and functional genomics in maize using fluorescent protein-tagged lines. *Plant Physiol.* **149,** 601–605 (2009).
28. Chen, J. G., Gao, Y. & Jones, A. M. Differential roles of *Arabidopsis* heterotrimeric G-protein subunits in modulating cell division in roots. *Plant Physiol.* **141,** 887–897 (2006).
29. Dennehey, B. K., Retersen, W. L., Ford-Santino, C., Pajeau, M. & Armstrong, C. L. Comparison of selective agents for use with the selectable marker gene *bar* in maize transformation. *Plant Cell Tissue Organ Cult.* **36,** 1–7 (1994).
30. Harlow, E. & Lane, D. *Antibodies: A Laboratory Manual*. (Cold Spring Harbor Laboratory Press, 1988).
31. Larsson, C. & Widell, S. in *Aqueous Two-Phase Systems: Methods and Protocols* Vol. 11 *Methods in Biotechnology*, (ed Hatti-Kaul, R.) 159–166 (Humana Press, 2000).

32. McDonald, W. H., Ohi, R., Miyamoto, D. T., Mitchison, T. J. & Yates. J. R. III. Comparison of three directly coupled HPLC MS/MS strategies for identification of proteins from complex mixtures: single-dimension LC-MS/MS, 2-phase MudPIT, and 3-phase MudPIT. *Int. J. Mass Spectrom.* **219,** 245–251 (2002).
33. Taylor, P. *et al.* Automated 2D peptide separation on a 1D nano-LC-MS system. *J. Proteome Res.* **8,** 1610–1616 (2009).
34. Washburn, M. P., Wolters, D. & Yates, J. R., III. Large-scale analysis of the yeast proteome by multidimensional protein identification technology. *Nature Biotechnol.* **19,** 242–247 (2001).

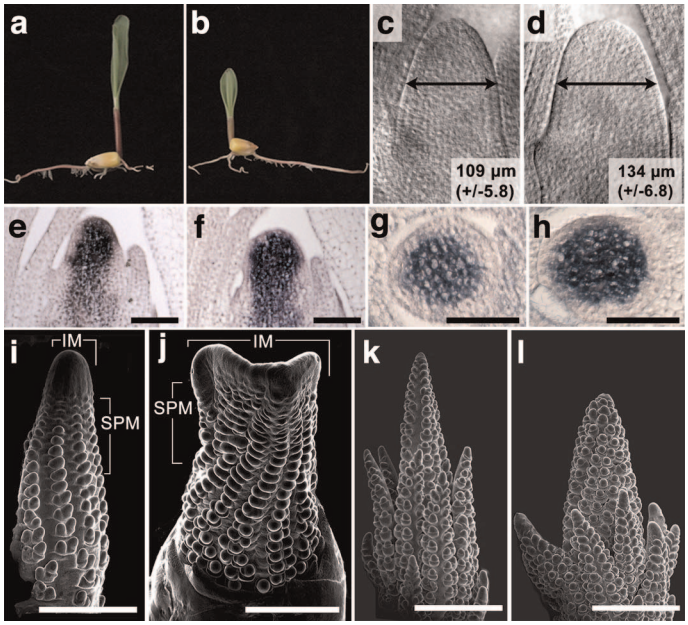

Extended Data Figure 1 | Phenotypic analysis of *ct2* mutants. **a**, Wild-type seedling. **b**, *ct2* seedling showing reduced height. **c**, Cleared wild-type vegetative SAM. **d**, Cleared *ct2* vegetative SAM showing increased diameter (± denotes s.d.; $n = 10$ for each genotype). **e**, Wild-type SAM longitudinal section probed *in situ* for *KNOTTED1* (*KN1*) mRNA. **f**, *ct2* SAM longitudinal section probed *in situ* for *KN1* mRNA showing a wider expression domain but normal patterning. **g**, **h**, Transverse sections of wild-type and *ct2* SAM probed *in situ* for *KN1*. **i**, SEM of wild-type ear primordium showing a regular shaped inflorescence meristem (IM) and regular arrangement of spikelet pair meristems (SPM) on the flanks. **j**, *ct2* ear primordium showing fasciation of the inflorescence meristem and irregular arrangement of SPM. **k**, Wild-type tassel primordium. **l**, *ct2* tassel primordium showing reduced length of main rachis and tassel branches and increased spikelet density. Scale bars represent 100 µm (**e**–**h**), 1 mm (**i**, **j**) and 2 mm (**k**, **l**).

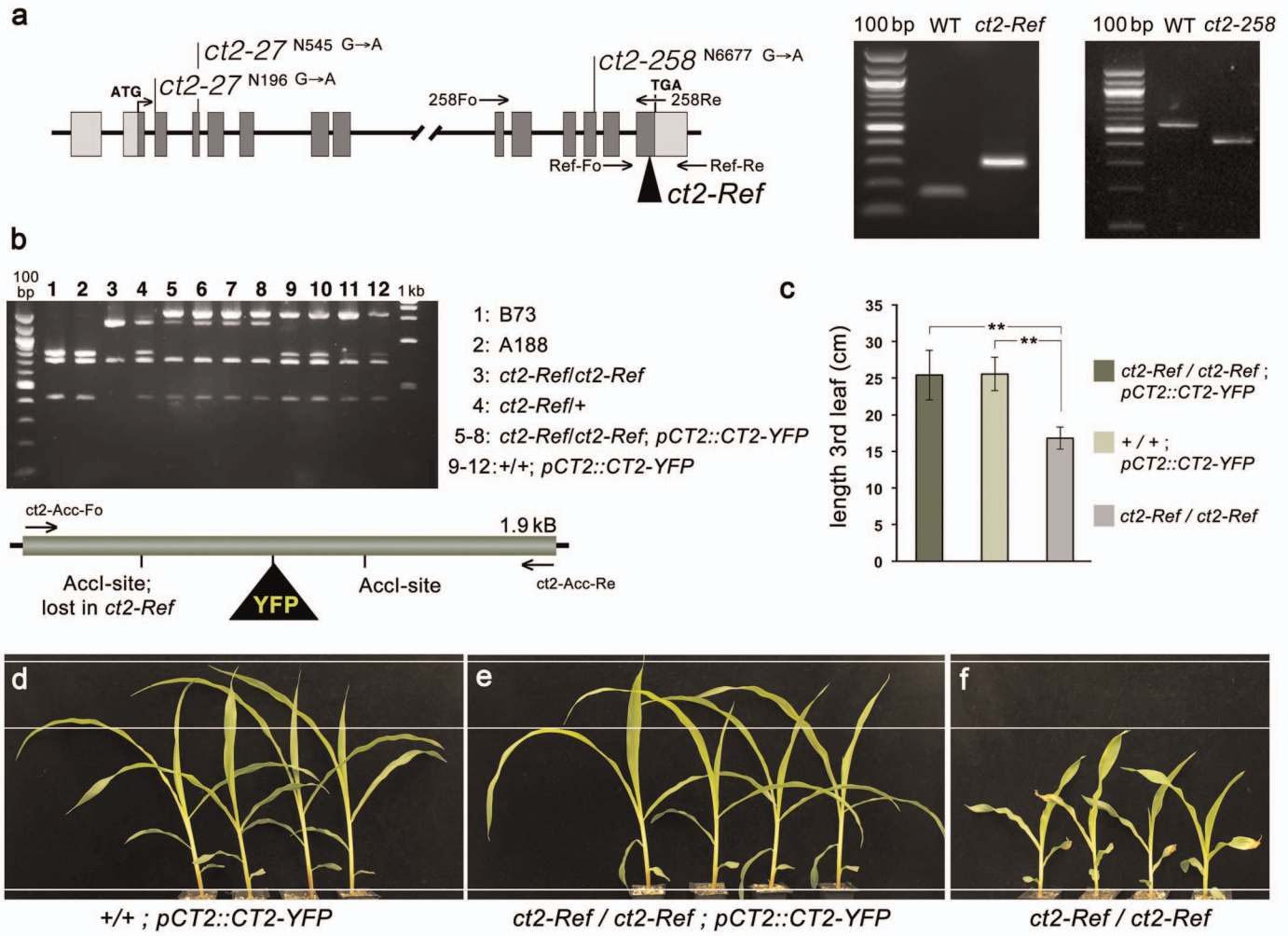

Extended Data Figure 2 | *ct2* alleles and complementation by the CT2–YFP transgene. **a**, Schematic of the *ct2* locus with mutations marked and agarose gel electrophoresis of partial *ct2-Ref* (left) and *ct2-258* (right) complementary DNA (cDNA) fragments compared to the corresponding wild type. cDNA fragments show increased size for the *ct2-Ref* allele owing to the insertion within exon 14, and reduced size for the *ct2-258* allele owing to skipping of exons 12 and 13. Primer locations are indicated in **a**. All 3 EMS induced alleles had mutations that induced aberrant splicing, which led to the introduction of premature stop codons. *ct2-258*, had a G to A transition at the last nucleotide of exon 12, disrupting the 5′ splice site of exon 12. This mutation caused skipping of exons 12 and 13. The G to A transition at the last nucleotide of exon 4 of the *ct2-2* allele disrupted the natural 5′ splice site, resulting in activation of a cryptic 5′ splice site five nucleotides downstream. Another G to A transition at the last nucleotide of intron 2 in the *ct2-27* allele disrupted the natural 3′ splice site generating a frame-shifted mRNA missing the first seven nucleotides of exon 3. **b**, *ct2* and CT2–YFP transgene genotyping. The genotyping scheme relies on an AccI site single nucleotide polymorphism that is lost in *ct2-Ref* and amplification of the YFP insertion in the transgene, as described in the Methods. **c**, Leaf length was indistinguishable between transgenic, homozygous *ct2-Ref* and wild-type plants, but significantly longer than non-transgenic *ct2-Ref* homozygous mutants (P value = 0.001, Student's t test; $n = 10$ for each genotype; error bars represent s.d.), indicating complementation. **d**, Seedling phenotypes of transgenic, wild-type plants. **e**, Seedling phenotype of transgenic, homozygous *ct2-Ref* plants. **f**, Seedling phenotype of non-transgenic, homozygous *ct2-Ref* plants; plants are dwarfed and develop shorter leaves. Pictures **d**–**f** are shown at identical magnification.

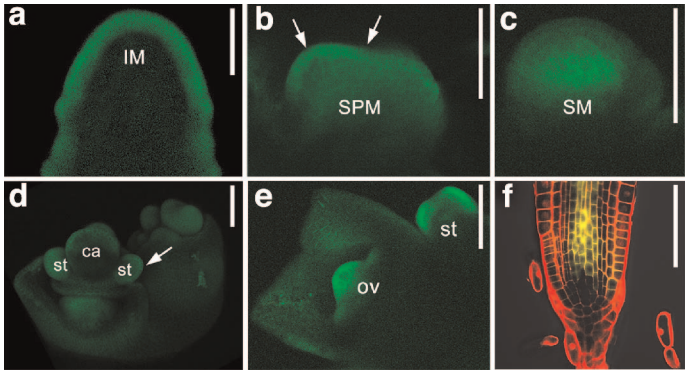

Extended Data Figure 3 | CT2–YFP expression. **a**, CT2–YFP expression in median optical section of the inflorescence meristem (IM) of an ear primordium, note expression is enhanced in outer layers. **b**, CT2–YFP expression in a spikelet pair meristem (SPM), showing enhanced expression in the L1 (arrows). **c**, More centrally localized CT2–YFP expression within a developing spikelet meristem (SM). **d**, CT2–YFP expression during early stages of floral development, in stamen (st) and carpel (ca) primordia. In both organs, YFP signal is enhanced in the L1 layer (arrow). **e**, Expression during ovule development, in the ovule (ov) and in the outer cell layers of the stamen primordia (st). **f**, CT2–YFP expression in roots that were counterstained with propidium iodide is localized along the cell periphery. Image **e** is a three-dimensional reconstruction of a *Z*-stack series; scale bars, 100 μm.

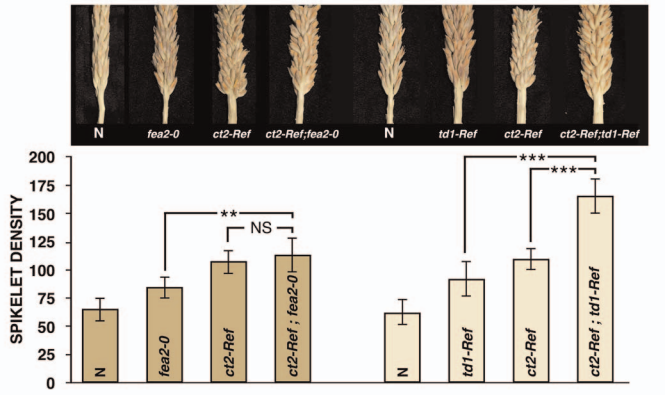

Extended Data Figure 4 | *ct2* double mutant analysis. Spikelet density of *ct2-Ref; td1-Ref* double mutants was significantly higher than either single mutant (***P value = 0.0001; Student's t test). In contrast, spikelet density in *ct2-Ref; fea2-0* double mutants was not significantly different (NS) from that of *ct2* single mutants (P value = 0.42; Student's t test), even though each single mutant was significantly higher than normal (P value = 0.001; Student's t test). However, *fea2* mutants were significantly different from *ct2;fea2* double mutants (**P value 0.001; Student's t test), suggesting that *CT2* also signals independently of *FEA2* in control of spikelet density; $n \geq 10$ for each genotype; error bars represent s.d. This experiment was conducted with 2 independent biological replicates.

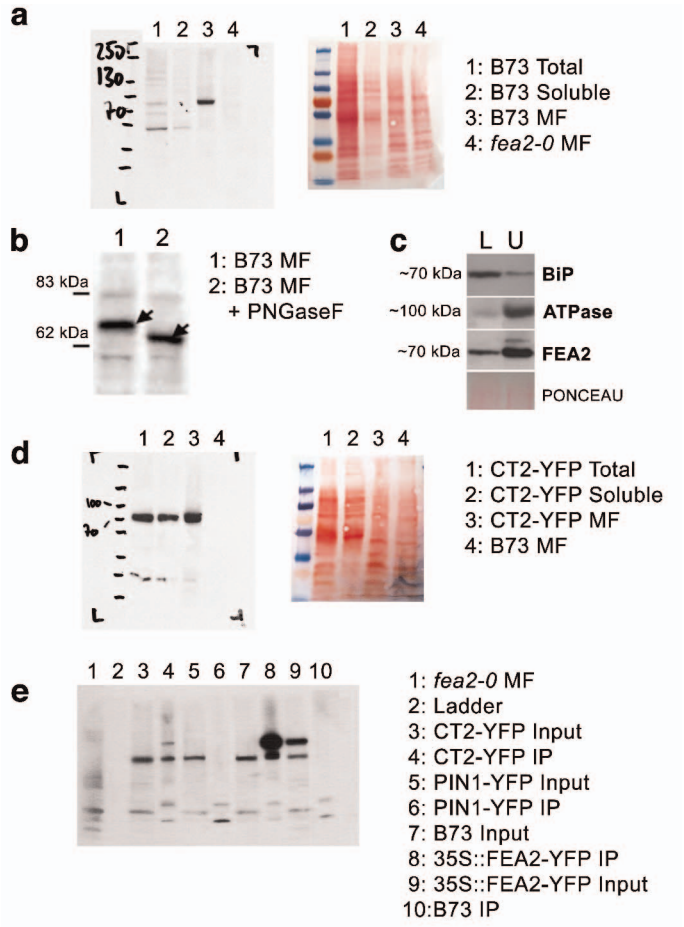

Extended Data Figure 5 | Full fractionation western blots and loading controls and FEA2 glycosylation and localization. **a**, Western blot probed with an anti-FEA2 peptide antibody and a secondary HRP-coupled antibody (GE); loading quantities shown on right side by 0.1% Ponceau S stain. The anti-FEA2 peptide antibody detects a band of ~70 kDa in B73 membrane enriched fractions (lane 3). Specificity of the antiserum is evident by the lack of a cross-reacting band in the membrane-enriched fraction from *fea2* ears (lane 4). **b**, FEA2 is glycosylated. It runs at ~70 kDa in B73 membrane-enriched fractions (lane 1) and is reduced in size upon treatment with PNGaseF glycosidase (lane 2). **c**, Subcellular fractionation of FEA2 by aqueous two-phase partitioning. The lower (L) and upper (U) phase fractions from B73 inflorescences were resolved on a 10% SDS–PAGE gel, and probed with antisera against BiP lumenal binding protein, or plasma membrane H^+ ATPase (Agrisera), or FEA2. Similar loading is shown by Ponceau staining. The endogenous FEA2 distribution is similar to the plasma membrane H^+ ATPase, suggesting that it localizes predominantly to the plasma membrane. **d**, Western blot probed with an anti-GFP peptide antibody and a secondary HRP coupled antibody (GE), loading quantities shown on right side by 0.1% Ponceau S stain. **e**, Complete scan of the IP western blot shown in Fig. 3d, showing full fractionation and all lanes on same gel. The blot was probed with an anti-FEA2 peptide antibody and a secondary HRP coupled antibody (GE). MF, membrane fraction. This experiment was conducted with 3 biological replicates.

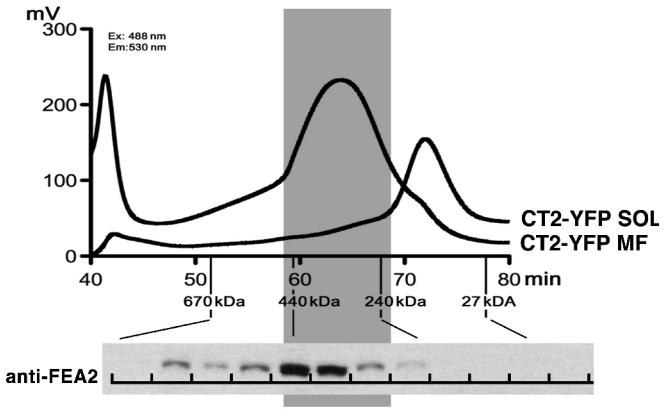

Extended Data Figure 6 | Overlapping sizes of FEA2 and CT2 protein complexes. In the lower panel, membrane enriched extracts from wild-type ears were fractionated by gel filtration, and fractions separated by SDS–PAGE and probed with the FEA2 antiserum. FEA2 was detected in complexes ranging from ~350 to 550 kDa, with a peak around 400 kDa. The positions of the marker proteins are indicated. In the upper panel, the CT2–YFP fusion protein was detected by spectroscopy as it eluted from the column. In cytoplasmic extracts, CT2–YFP in the soluble fraction (CT2–YFP SOL) eluted at ~100 kDa, suggesting an interaction with unknown cytoplasmic protein(s). In contrast, a membrane-enriched fraction (CT2–YFP MF) showed that CT2–YFP membrane complexes were a broad range of sizes that overlapped with the FEA2 complex size at ~400 kDa (shaded area).

Extended Data Table 1 | *ct2* mutant leaves are shorter and wider but cell size is not significantly different.

	blade length* (cm)	blade width† (cm)	number of cell files‡	cell lengths§ (μm)
wt	34.95 (2.41)	2.37 (0.13)	358 (10)	103.8 (7.3)
ct2	24.11‖ (1.54)	2.85‖ (0.17)	358¶ (12)	117.9¶ (12.6)

Numbers are mean values with standard deviations in parentheses; measurements made on 18-day-old seedlings, using the fourth leaf. *Length measured from blade tip to blade-sheath boundary; $n = 17$.†Blade width measured at middle of each blade; $n = 17$.‡Number of cell files per cm across the leaf; $n = 5$. §Cell size along the longitudinal (proximo–distal) leaf axis; each measurement represents the average of 5 adjacent cells; $n = 6$. ‖Significant difference from WT: P value = 0.01, Student's t test. ¶Insignificant difference from WT: P value >0.1, Student's t test.